

# Two-Dimensional Nuclear Magnetic Resonance Spectroscopy

By James Keeler

DEPARTMENT OF CHEMISTRY, UNIVERSITY OF CAMBRIDGE,  
LENSFIELD ROAD, CAMBRIDGE, CB2 1EW

## 1 Introduction

It is hardly possible to open an issue of any current chemical journal without being presented with several two-dimensional NMR spectra. The ubiquity of such spectra shows that the technique has now moved from the realm of a few specialist users to being a widely available and appreciated tool for structural studies. Two-dimensional spectra are even beginning to make an appearance on University examination papers, a further sign that the technique is now firmly established. The purpose of this review is to describe firstly how two-dimensional NMR spectra are used in structural studies and secondly the principles behind the experiments used to record such spectra. The approach adopted will be non-mathematical and it will be assumed that the reader has a basic knowledge of conventional proton and carbon-13 NMR spectroscopy.

A very great number of different two-dimensional NMR experiments have been devised and it would be both impossible and unprofitable to describe even a fraction of these in the present work. However, there are only a few basic principles involved and these can be illustrated by reference to a small number of experiments. Fortunately, it turns out that these basic experiments are also the most widely used ones. For further information on these techniques and their applications there is a large number of specialized reviews and books available. Some approach the topic from the point of view of the chemical information obtainable from such techniques,<sup>1–3</sup> others adopt a more physicochemical view,<sup>4–7</sup> and finally there are advanced texts which adopt a strict quantum mechanical approach to the subject.<sup>8,9</sup>

## 2 Two-Dimensional NMR in Action

**A. Assignment of Spectra.**—To be of any use to us an NMR spectrum must first be *assigned*, which means working out which peaks are associated with which

<sup>1</sup> J. K. M. Sanders and B. K. Hunter, 'Modern NMR Spectroscopy', OUP, 1987.

<sup>2</sup> A. E. Derome, 'Modern NMR Techniques for Chemical Research', Pergamon Press, 1987.

<sup>3</sup> R. Benn and H. Günther, *Angew. Chem., Int. Ed. Engl.*, 1983, **22**, 350.

<sup>4</sup> G. A. Morris, *Magn. Reson. Chem.*, 1986, **24**, 371.

<sup>5</sup> H. Kessler, M. Gehrke, and C. Griesinger, *Angew. Chem., Int. Ed. Engl.*, 1988, **27**, 490.

<sup>6</sup> N. Chandrakumar and S. Subramanian, 'Modern Techniques in High-Resolution FT-NMR', Springer-Verlag, 1987.

<sup>7</sup> A. Bax, 'Two-Dimensional Nuclear Magnetic Resonance in Liquids', Delft University Press, 1982.

<sup>8</sup> R. R. Ernst, G. Bodenhausen, and A. Wokaun, 'Principles of Nuclear Magnetic Resonance in One and Two Dimensions', OUP, 1987.

<sup>9</sup> M. Goldman, 'Quantum Description of High-Resolution NMR in Liquids', OUP, 1988.

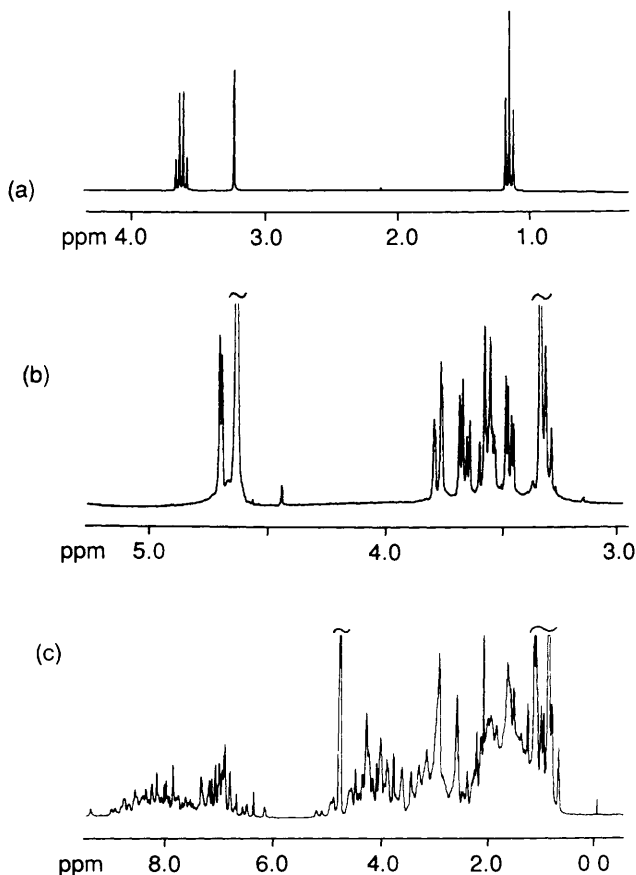
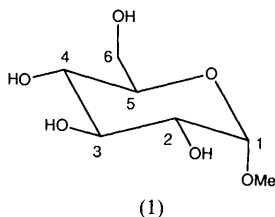


**Figure 1** Proton NMR spectra of three molecules of differing complexity (a) the spectrum of ethanol which can be assigned by simple chemical shift arguments, (b) the spectrum of 1-O-methyl  $\alpha$ -D-glucopyranoside (1) (recorded at 400 MHz) which can be partially assigned by simple arguments, (c) the spectrum (recorded at 500 MHz) of two 'zinc fingers' from SW15, a transcription activator protein of molecular weight ca 7000 isolated from yeast. The spectrum of even such a relatively small protein can only be assigned with the aid of a whole armoury of two-dimensional NMR techniques (SW15 spectrum kindly provided by David Neuhaus, MRC, LMB, Cambridge)

hydrogens in the structure. Once this has been done, more information can be extracted, such as the values of couplings which give conformational information (for example *via* the Karplus equation). An assignment is also crucial in interpreting the results of other NMR experiments, such as nuclear Overhauser effect (NOE) or relaxation time studies. If the structure is unknown, the spectroscopist attempts to fit the spectrum to a series of trial structures until a consistent assignment is found.

Figure 1 shows the proton spectra of three molecules of greatly differing



complexity. The first, Figure 1 (a), is the spectrum of ethanol which can be assigned simply on the basis of arguing that, due to the presence of the electronegative oxygen substituent, the methylene protons should appear at lower field than the methyl protons. The spectrum from 1-*O*-methyl  $\alpha$ -D-glucopyranoside, compound (1), shown in Figure 1 (b) is rather more complex. Certain resonances can be assigned on the basis of shift arguments, for example the anomeric proton is easily identified, as is the characteristically sharp methyl resonance. A complete assignment could not be made from this spectrum alone, however it will be shown below that such an assignment can be made with the aid of one two-dimensional experiment. Further, a second two-dimensional experiment will enable us to assign the carbon-13 spectrum as well. Finally, in Figure 1 (c) is shown the proton spectrum of a 'zinc finger' protein. The spectrum is complex because it contains very many overlapping lines and the assignment of such a spectrum is a challenging and complex procedure even with the aid of two-dimensional NMR.

**B. COSY.**—The spectrum of (1) can be assigned with the aid of a two-dimensional COSY spectrum. COSY stands for COReLation Spectroscopy.<sup>10,11</sup> At this point attention will be focused on the appearance and interpretation of such a spectrum, later the way in which the experiment actually works will be discussed.

Conventional NMR spectra (one-dimensional spectra) are plots of intensity *vs.* frequency; in two-dimensional spectroscopy intensity is plotted as a function of two frequency axes usually called  $F_1$  and  $F_2$ . There are various ways of representing such a spectrum on paper, but the one most usually used is to make a contour plot in which the intensity of the peaks is represented by contour lines drawn at suitable intervals, in the same way as a topographical map. The position of each peak is specified by two frequency co-ordinates corresponding to  $F_1$  and  $F_2$ . Two-dimensional NMR spectra are always arranged so that the  $F_2$  co-ordinates of the peaks correspond to those found in the normal one-dimensional spectrum, and this relation is often emphasized by plotting the one-dimensional spectrum alongside the  $F_2$  axis.

Figure 2 shows a schematic COSY spectrum of a hypothetical molecule

<sup>10</sup> W. P. Aue, E. Bartholdi, and R. R. Ernst, *J. Chem. Phys.*, 1976, **64**, 2229.

<sup>11</sup> A. Bax and R. Freeman, *J. Magn. Reson.*, 1981, **44**, 542.

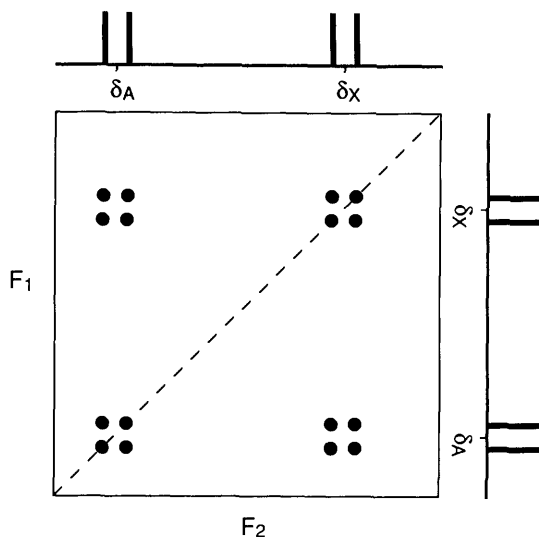


**Figure 2** Schematic COSY spectrum of a two coupled spins denoted *A* and *X*. For convenience the normal one-dimensional spectrum is plotted alongside the  $F_1$  and  $F_2$  axes and the diagonal ( $F_1 = F_2$ ) is indicated by a dashed line. This spectrum shows two types of multiplets: those centred at the same  $F_1$  and  $F_2$  frequencies called diagonal-peak multiplets and those centred at different frequencies in the two dimensions called cross-peak multiplets. Each multiplet has four component peaks. The appearance of a cross-peak multiplet centred at  $F_1 = \delta_A$ ,  $F_2 = \delta_X$  indicates that the proton with shift  $\delta_A$  is coupled to the proton with shift  $\delta_X$ . This observation is all that is required to interpret a COSY spectrum.

containing just two protons, *A* and *X*, which are coupled together with a scalar coupling of  $J_{AX}$  Hz. The one-dimensional spectrum is plotted alongside the  $F_2$  axis, and consists of the familiar pair of doublets centred on the chemical shifts of *A* and *X*,  $\delta_A$  and  $\delta_X$  respectively. In the COSY spectrum the  $F_1$  co-ordinates of the peaks in the two-dimensional spectrum also correspond to those found in the normal one-dimensional spectrum and to emphasize this point the one-dimensional spectrum has been plotted alongside the  $F_1$  axis. It is immediately clear that this COSY spectrum has some symmetry about the diagonal  $F_1 = F_2$  which has been indicated with a dashed line.

In a one-dimensional spectrum scalar couplings give rise to multiplets in the spectrum, which are described by the familiar terms doublet, triplet, doublet of doublets *etc*. In two-dimensional spectra the idea of a multiplet has to be expanded somewhat so that in such spectra a multiplet consists of an array of individual peaks often giving the impression of a square or rectangular outline. Several such arrays of peaks can be seen in the schematic COSY spectrum of Figure 2. These two-dimensional multiplets come in two distinct types: *diagonal-peak multiplets* which are centred around the same  $F_1$  and  $F_2$  frequency co-ordinates and *cross-peak multiplets* which are centred around different  $F_1$  and  $F_2$  co-ordinates. Thus in the schematic COSY spectrum there are two diagonal-peak

multiplets centred at  $F_1 = F_2 = \delta_A$  and  $F_1 = F_2 = \delta_X$  one cross-peak multiplets centred at  $F_1 = \delta_A, F_2 = \delta_X$  and a second cross-peak multiplet centred at  $F_1 = \delta_X, F_2 = \delta_A$ .

The appearance in a COSY spectrum of a cross-peak multiplet  $F_1 = \delta_A, F_2 = \delta_X$  indicates that the two protons at shifts  $\delta_A$  and  $\delta_X$  have a scalar coupling between them. This statement is all that is required for the analysis of a COSY spectrum, and it is this simplicity which is the key to the great utility of such spectra. From a single COSY spectrum it is possible to trace out the whole coupling network in the molecule. This important point is best illustrated by moving to a hypothetical molecule which has three coupled protons, A, M, and X. Figure 3 shows schematic COSY spectra of such a three spin system for two cases: in (a) the spectrum is shown for the case of A coupled to M, and M coupled to X but with no coupling between A and X. In Figure 3 (b) the spectrum is shown for the case where all three protons are coupled to one another. As in the case of the two-spin system, both spectra show the uninformative diagonal-peak multiplets, as well as several cross-peak multiplets.

In Figure 3 (a) there are cross-peak multiplets at  $F_1 = \delta_A, F_2 = \delta_M$  and  $F_1 = \delta_M, F_2 = \delta_X$  indicating that proton A is coupled to M, and M is coupled to X. However, there is no cross-peak multiplet at  $F_1 = \delta_A, F_2 = \delta_X$  indicating that protons A and X are not coupled. In contrast, the spectrum of Figure 3 (b) shows cross-peak multiplets between all three spins. Thus, from the COSY spectrum it is possible to deduce the *topology* of the coupling network between the protons. The spectrum of Figure 3 (a) indicates a linear arrangement of spins, whereas in (b) the topology is a triangular arrangement. Since couplings are transmitted through bonds, tracing out the topology is very closely related to tracing out the molecular framework. Diagonal-peak multiplets do not give any extra information, but their presence in the spectrum is useful in that they make for an eye-catching symmetry which allows correlations to be identified readily.

For more complex molecules the COSY spectrum can be interpreted in just the same way as the simple systems described above; the rule is simply that a cross-peak multiplet indicates a coupling. If there is no cross-peak multiplet there is no coupling. Figure 4 shows the COSY spectrum of 1-*O*-methyl  $\alpha$ -D-glucopyranoside, (1). It is immediately clear that there are several cross-peak multiplets present, as well as an easily recognizable series of diagonal-peak multiplets. Parts of the spectrum look rather different to the schematic COSY spectra of Figure 3. The reason for this is that the resolution in the experimental COSY spectrum is not always sufficient to separate clearly all the individual peaks which form a cross- or diagonal-peak multiplet. As they merge together the two-dimensional multiplets take on the appearance of a square or rectangular blob. This loss of resolution does not result in the loss of any information, as a cross-peak multiplet, even if just a blob, still indicates the presence of a coupling.

The spectrum of (1) contains some features that we can identify at once. The sharp resonance at 3.3 ppm is clearly the OMe group, and the lowest field multiplet, H, is easily identified as the anomeric proton, H1, on the basis of its

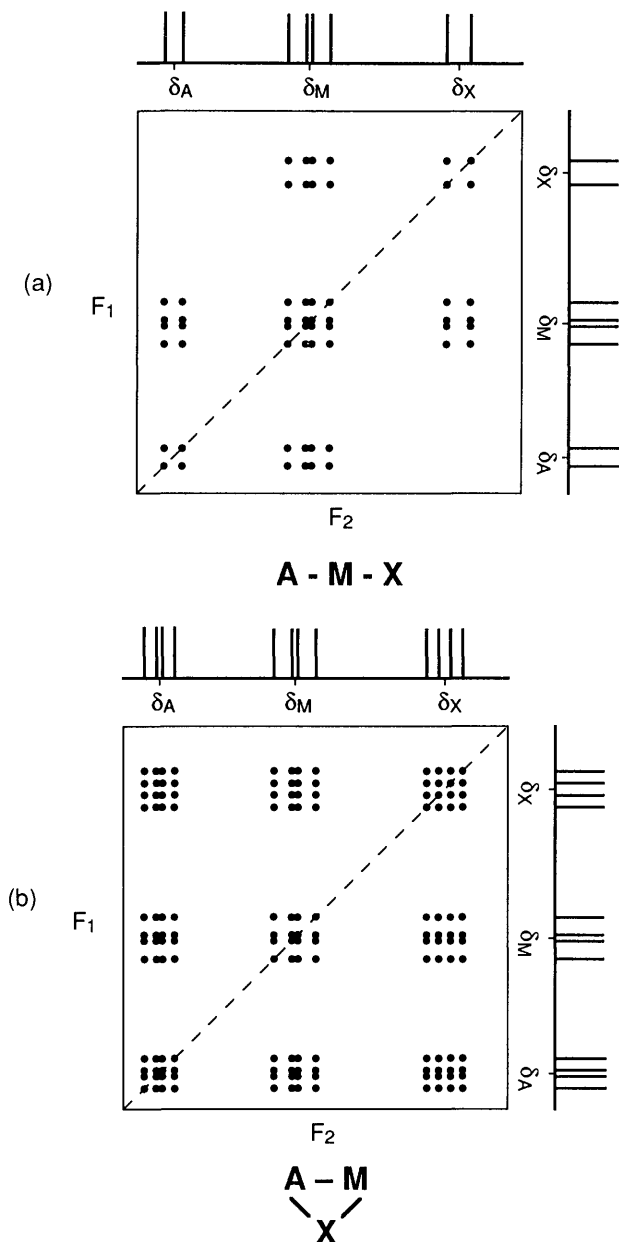


**Figure 3** Schematic COSY spectra for a three spin system *AMX* with two different coupling topologies. Spectrum (a) is appropriate for the case where spin *A* is coupled to *M*, *M* is coupled to *X* but where there is no coupling between *A* and *X*. The presence of cross-peak multiplets at  $F_1 = \delta_A$ ,  $F_2 = \delta_M$  and  $F_1 = \delta_M$ ,  $F_2 = \delta_X$  together with the absence of a cross-peak multiplet centred at  $F_1 = \delta_A$ ,  $F_2 = \delta_X$  confirms this linear coupling topology. Spectrum (b) is appropriate for the case where all three spins are coupled to one another as there are cross-peaks indicating each of these couplings. A triangular topology of couplings is indicated as shown under the spectrum.

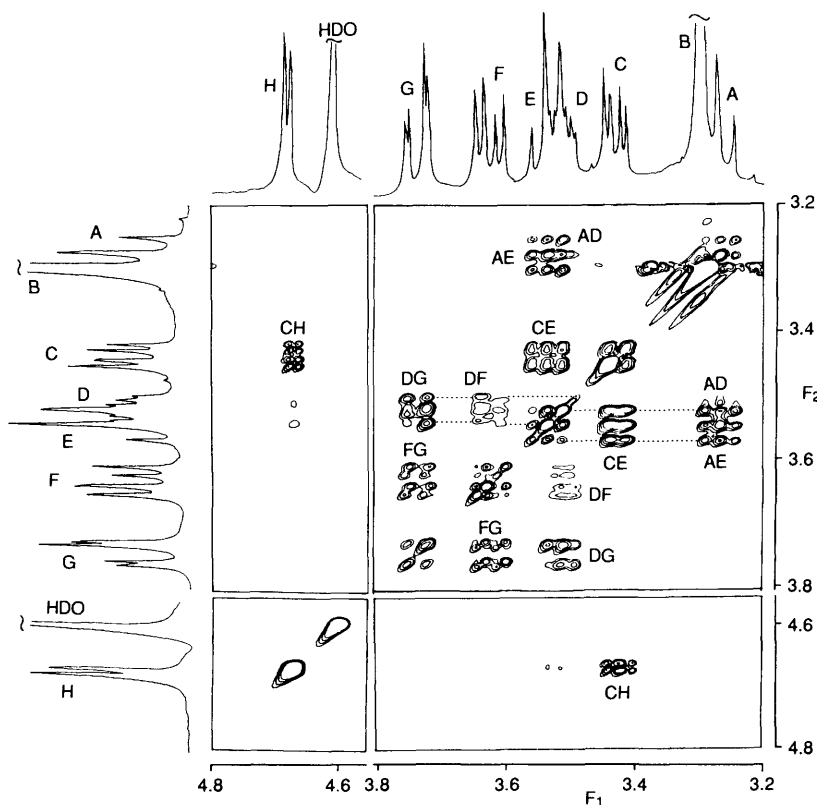


**Figure 4** COSY spectrum of 1-O-methyl  $\alpha$ -D-glucopyranoside, (1), recorded at 400 MHz. For convenience the conventional proton spectra have been plotted alongside the  $F_1$  and  $F_2$  axes and a blank part of the spectrum has not been plotted; the tops of intense peaks have been truncated. Each proton multiplet in the conventional spectrum is assigned a letter and the cross-peak multiplets are labelled with two letters to indicate which two proton multiplets are responsible for the cross-peak. The logic behind the assignment is described in the text. Note that the  $F_1$  axis is horizontal in this spectrum, in contrast to Figures 2 and 3 in which the  $F_2$  axis is horizontal

characteristic chemical shift. With the aid of the COSY spectrum of Figure 4 it is possible to assign this spectrum by using the anomeric proton as a starting point and following the series of three-bond couplings round the molecule. Multiplet H shows a clear cross-peak to C, identifying C as H<sub>2</sub>. Multiplet C shows a cross-peak to E, identifying the latter as H<sub>3</sub>. Multiplet E shows a cross-peak to the highest field multiplet, A, which is partly obscured by the OMe resonance. We thus identify multiplet A as being from H<sub>4</sub>. Multiplet A shows a cross-peak to D, although this is somewhat obscured by the stronger cross-peak between A and E; D is therefore identified as H<sub>5</sub>. Finally, D shows cross-peaks with both F and G, while F and G also show a cross-peak between them, thus F and G are the

two methylene protons 6 and 6. The only slight difficulty with this assignment is in recognizing which of the multiplets E and D a particular cross-peak correlates with. Careful inspection of the spectrum will show that the cross-peaks marked AE and CE align with one another and not with the cross-peaks marked DG and DF, dotted lines have been added to aid in this distinction. Thus, the COSY spectrum has enabled us to follow the chain of couplings round the molecule and find a complete assignment.

The description and use of a COSY spectrum for assigning an NMR spectrum has revealed many of the features which make two-dimensional NMR such a powerful tool. In particular, the information in such a spectrum is presented in a readily appreciable and unambiguous manner. A second feature, which has gone unremarked so far, is that the multiplets in the two-dimensional spectrum are dispersed into a much wider area of frequency space than they are in a one-dimensional spectrum. This gives two-dimensional spectra a much greater effective resolution than their one-dimensional counterparts. The COSY spectrum of Figure 4 is an illustration of this point: multiplet A is overlapped with the OMe resonance in the one-dimensional spectrum, but in the COSY the triplet structure of the A multiplet is easily discerned from the cross-peak multiplet AE. Likewise the overlapping multiplets E and D give rise to distinct separated cross-peaks. This increase in effective dispersion obtained in two-dimensional spectra is much larger than can be achieved by going to even the highest magnetic field strengths.

### **3 The Mechanics of Two-Dimensional Experiments**

**A. Pulse Fourier Transform NMR.**—In conventional optical spectroscopy light is passed through a sample and its absorption recorded as the wavelength of the light is scanned through the region of interest. Originally NMR spectra were recorded in much the same way by sweeping a radio-frequency transmitter through the spectrum. However a far better way of recording such spectra is to use a version of the experiment known as pulse Fourier transform NMR.<sup>12</sup>

In a pulsed NMR experiment the sample is subjected to a very intense pulse of radio-frequency power, typically only lasting a few microseconds. This pulse causes the nuclear spins to ring much in the same way that a bell rings when it is struck. The ringing signal, called a free induction decay, is recorded as a function of time, a typical example of such a signal is shown in Figure 5 (a).

The free induction decay is not useful directly to the spectroscopist as it is a plot of intensity as a function of time, rather than as a function of frequency. If there is only one line in the spectrum the free induction decay looks rather simple as it is just a cosine wave which gradually dies away. If there are two lines in the spectrum, the free induction decay is the sum of two decaying cosines of different frequencies which gives rise to a beat pattern. However, a spectrum consisting of perhaps hundreds of lines gives a free induction decay that is a hopeless jumble. Luckily there is a mathematical operation, called Fourier transformation, which

<sup>12</sup> R. K. Harris, *Nuclear Magnetic Resonance Spectroscopy*, Longman, 1983.



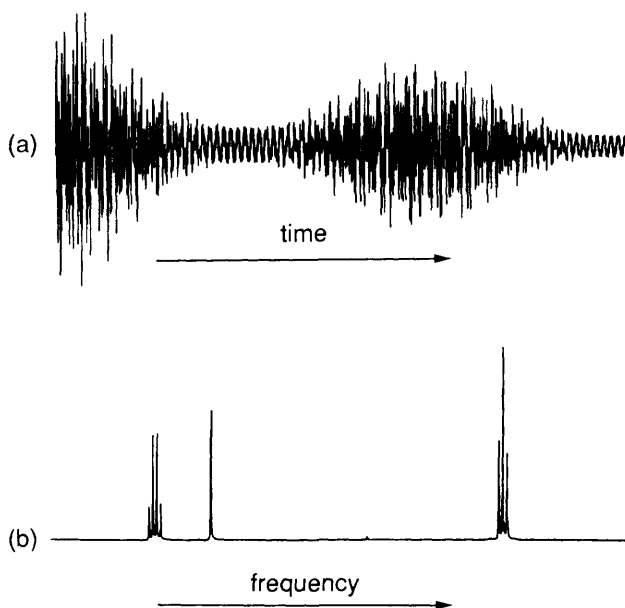


**Figure 5** A typical free induction decay (a) obtained when a sample is excited with a short pulse of radio-frequency power, and the corresponding spectrum (b) obtained by Fourier transformation of (a). The free induction decay is a function of time and consists of a superposition of many cosine waves of different frequencies and amplitudes. Fourier transformation takes this data and converts it into the frequency domain in which the x and y co-ordinates of a point are the frequency and amplitude of a particular decaying cosine wave in the free induction decay

will turn the free induction decay into the familiar spectrum.<sup>13,14</sup> Essentially, the Fourier transform picks out the intensities of all the frequency components that are present in the free induction decay and reconstructs the information in the form of a spectrum. On modern computers this Fourier transformation is a trivial calculation taking just a few seconds. The result of transforming the time domain signal in Figure 5(a) is shown in (b): it is the familiar spectrum.

There are many reasons why pulsed Fourier transform NMR is superior to swept frequency NMR. The most important of these is that the whole spectrum is examined at once so that the technique is more time-efficient than sweeping through the spectrum; this results in higher sensitivity. In addition, more than one pulse can be applied to the sample so as to manipulate the nuclear spins in rather subtle ways. It will be seen in the following sections that such 'multiple pulse' NMR experiments are used to give two-dimensional spectra.

The free induction decay is transferred into the computer memory using an analog to digital converter (ADC). This device measures the amplitude of the

<sup>13</sup> R. N. Bracewell, 'The Fourier Transform and its Applications', Plenum, 1978.

<sup>14</sup> 'Transform Techniques in Chemistry', ed. R. Griffiths, Plenum, 1978.

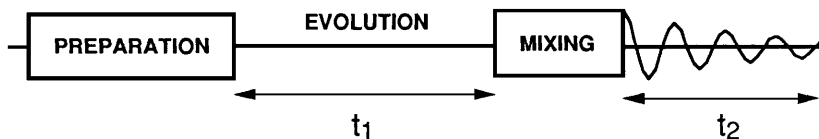


**Figure 6** The general scheme for two-dimensional NMR experiments. The NMR signal in the form of a free induction decay is recorded during the time  $t_2$ . This process is repeated for a series of values of  $t_1$ . During the preparation period one or more pulses are applied so as to generate a signal which will evolve during the time  $t_1$ . The mixing period consists of one or more pulses and it is the nature of the mixing process that determines how the evolution during  $t_1$  affects the signal observed during  $t_2$ .

NMR signal at a particular instant and converts this value into a digital format that the computer can store. The free induction decay is measured and digitized at regularly spaced intervals, the time between each sampling being the same. If this time between samples is  $\Delta$ , then the resulting spectrum covers a range of 0 to  $1/(2\Delta)$  Hz, this range is known as the spectral width. For example, a typical proton spectrum spans 10 ppm which, on a 250 MHz spectrometer, corresponds to a frequency range of  $10 \times 10^6 \times 250 \times 10^6 = 2500$  Hz. The sampling interval would be set to  $1/(2 \times 2500)$  or 200  $\mu$ s. The sampling process is carried on until the signal has decayed away, which is typically after a second or two.

**B. General Scheme for Two-Dimensional NMR.**—In one-dimensional pulsed Fourier transform NMR the signal is recorded as a function of one time variable and then Fourier transformed to give a spectrum which is a function of one frequency variable. In two-dimensional NMR the signal is recorded as a function of two time variables,  $t_1$  and  $t_2$ , and the resulting data Fourier transformed twice to yield a spectrum which is a function of two frequency variables. Figure 6 shows a general scheme for two-dimensional spectroscopy. In the first period, called the preparation time, the sample is excited by one or more pulses. The resulting signal is allowed to evolve for the first time period,  $t_1$ . Then another period follows, called the mixing time, which consists of a further pulse or pulses. After the mixing period the signal is recorded as a function of the second time variable,  $t_2$ . This sequence of events is called a *pulse sequence* and the exact nature of the preparation and mixing periods determines the information found in the spectrum.

It is important to realize that the signal is not recorded during the time  $t_1$ , but only during the time  $t_2$  at the end of the sequence. Just as was described above for one-dimensional spectroscopy, the data are recorded at regularly spaced intervals in both  $t_2$  and  $t_1$ .

The two-dimensional signal is recorded in the following way. First,  $t_1$  is set to zero, the pulse sequence is executed and the resulting free induction decay recorded. Then the nuclear spins are allowed to return to equilibrium, typically taking a few seconds to achieve this, and  $t_1$  is then set to  $\Delta_1$ , the sampling interval in  $t_1$ . The sequence is repeated and a free induction decay is recorded and stored separately from the first. Again the spins are allowed to equilibrate,  $t_1$  is set to

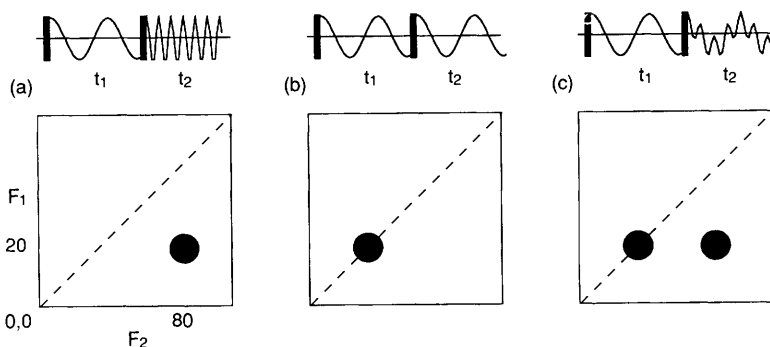
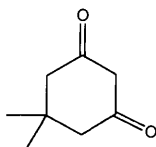


**Figure 7** Schematic two-dimensional spectra showing the interpretation of the co-ordinates of a peak in terms of the evolution during  $t_1$  and  $t_2$ . In spectrum (a) a peak appears at  $F_1 = 20\text{ Hz}$ ,  $F_2 = 80\text{ Hz}$ . This can be interpreted as being the result of a signal which evolved during  $t_1$  at  $20\text{ Hz}$  and which was then transferred, by some mixing process, to a signal that evolved at  $80\text{ Hz}$  during  $t_2$ . In spectrum (b) the peak has the same co-ordinates in each dimension and so comes from a signal whose frequency was unaffected by the mixing process. Finally, in spectrum (c) two peaks are seen with the same  $F_1$  frequency of  $20\text{ Hz}$ , but with  $F_2$  frequencies of  $20$  and  $80\text{ Hz}$ . Such an arrangement of peaks is the result of the mixing process partly transferring the signal to one which evolves at  $80\text{ Hz}$  during  $t_2$  and leaving part of it to continue evolving at  $20\text{ Hz}$  during  $t_2$ .

$2\Delta_1$ , the pulse sequence repeated and a free induction decay recorded and stored. The whole process is repeated again for  $t_1 = 3\Delta_1, 4\Delta_1$  and so on until sufficient data are recorded, typically 50 to 500 increments of  $t_1$ . Thus recording a two-dimensional data set involves repeating a pulse sequence for increasing values of  $t_1$  and recording a free induction decay as a function of  $t_2$  for each value of  $t_1$ .

**C. Interpretation of Peaks in a Two-Dimensional Spectrum.**—Within the general framework outlined in the previous section it is now possible to interpret the appearance of a peak in a two-dimensional spectrum at particular frequency co-ordinates. Suppose that in some unspecified two-dimensional spectrum a peak appears at  $F_1 = 20\text{ Hz}$ ,  $F_2 = 80\text{ Hz}$ . The interpretation of this peak is that a signal was present during  $t_1$  which evolved with a frequency of  $20\text{ Hz}$ . During the mixing time this *same* signal was transferred in some way to another signal which evolved at  $80\text{ Hz}$  during  $t_2$ . This is illustrated in Figure 7 (a). Likewise, if there is a peak at  $F_1 = 20\text{ Hz}$ ,  $F_2 = 20\text{ Hz}$  the interpretation is that there was a signal evolving at  $20\text{ Hz}$  during  $t_1$  which was unaffected by the mixing period and continued to evolve at  $20\text{ Hz}$  during  $t_2$ , as illustrated in Figure 7 (b). The processes by which these signals are transferred will be discussed in the following sections.

Finally, consider the spectrum shown in Figure 7 (c). Here there are two peaks, one at  $F_1 = 20\text{ Hz}$ ,  $F_2 = 80\text{ Hz}$  and one at  $F_1 = 20\text{ Hz}$ ,  $F_2 = 20\text{ Hz}$ . The interpretation of this is that some signal was present during  $t_1$  which evolved at



(2)

20 Hz and that during the mixing period part of it was transferred into another signal which evolved at 80 Hz during  $t_2$ . The other part remained unaffected and continued to evolve at 20 Hz. On the basis of the previous discussion of COSY spectra, the part that changes frequency during the mixing time is recognized as leading to a cross-peak and the part that does not change frequency leads to a diagonal-peak. This kind of interpretation is a very useful way of thinking about the meaning of peaks in a two-dimensional spectrum.

It is clear from the discussion in this section that the mixing time plays a crucial role in forming the two-dimensional spectrum. In the absence of a mixing time, the frequencies that evolve during  $t_1$  and  $t_2$  would be the same and only diagonal-peaks would appear in the spectrum. To obtain an interesting and useful spectrum it is essential to arrange for some process during the mixing time to transfer signals from one spin to another.

#### 4 EXCSY Spectra

EXCSY stands for EXChange Spectroscopy<sup>15</sup>. It is a two-dimensional NMR experiment which gives a spectrum in which the cross-peaks indicate which spins are undergoing mutual chemical exchange. This experiment will be illustrated using the exchange processes that take place in dimedone (2), whose one-dimensional spectrum and structure are shown in Figure 8. Figure 9 (a) shows the pulse sequence used to record EXCSY spectra and parts of the resulting two-dimensional spectrum of dimedone are shown in (b) and (c).

Dimedone undergoes a reversible keto-enol tautomerism in the conditions under which the spectrum was recorded, and this exchange is slow enough on the NMR timescale that distinct resonances are seen for both species. The assignment and a simple reaction scheme for the exchange process is shown in Figure 8. In the EXCSY spectrum there is a cross-peak at an  $F_1$  = shift of proton K1 and  $F_2$  = shift of proton E1, indicating that these two protons are exchanging. In addition, there are cross-peaks between the methyl resonances E3 and K3, and between the ring methylene resonances E2 and K2, further confirming the nature of the exchange process. Turning now to the H<sub>2</sub>O/OH peak, this is seen to have a cross-peak with the keto proton, K1 but no cross-peak with E1. This observation implies that K1 exchanges directly with the water, but E1 does not. This spectrum thus provides, in a very simple way, a great deal of information about the exchange processes that are taking place in this molecule. In this

<sup>15</sup> J Jeener, B H Meier, P Bachmann and R R Ernst *J Chem Phys* 1979 71 4546

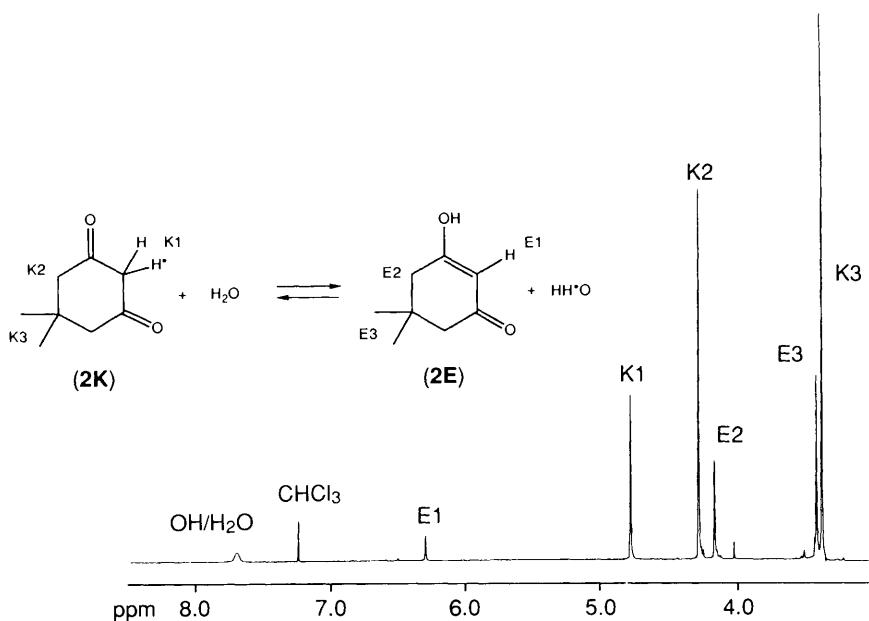


**Figure 8** Proton spectrum of dimedone (2) recorded at 250 MHz. Under the conditions in which this spectrum was recorded, dimedone undergoes a slow interconversion between a keto and an enol form, (2K) and (2E) respectively, as indicated by the reaction scheme. The assignment of resonances to individual protons in the two species is indicated on the spectrum

simple case, it simply confirms our existing chemical intuition, but in more complex cases involving fluxional molecules or complex reactions, EXCSY spectra provide invaluable insight into the nature of the chemical processes taking place. In the same way that COSY provides an almost visual map of the coupling network, EXCSY provides a similar map of the exchange processes taking place.

The EXCSY experiment has been chosen at this point as it is possible to explain the detailed form of the two-dimensional experiment without recourse to quantum mechanics. The experiment can be described with reference to a simple vector picture of pulsed NMR. It is not possible to describe fully or justify this simple picture within this review (details can be found in other places),<sup>12,16</sup> but for the present purposes some rules for the manipulation of these vectors can be stated:

- (i) Each separate spin in the molecule gives rise to a magnetization vector.
- (ii) At equilibrium these magnetization vectors lie along the direction of the applied magnetic field, conventionally taken as  $z$ .

<sup>16</sup> R. Freeman, 'A Handbook of Nuclear Magnetic Resonance', Longman, 1988.

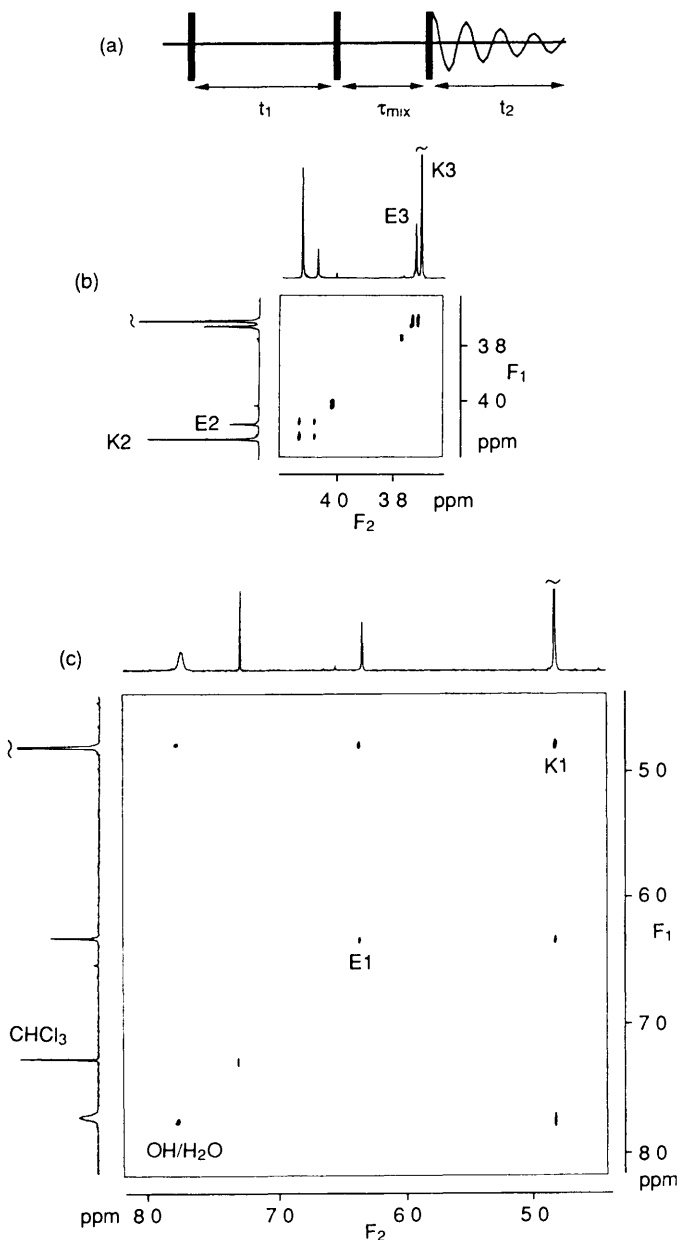


**Figure 9** (a) Pulse sequence used to record two-dimensional EXSY spectra (b) and (c) parts of the EXSY spectrum of dmedone (2). For convenience the conventional proton spectrum has also been plotted alongside the  $F_1$  and  $F_2$  axes and the two regions have been plotted on different scales. The presence of a cross-peak in the EXSY spectrum at  $F_1 = \delta_A$ ,  $F_2 = \delta_B$  indicates that the spins resonating at  $\delta_A$  and  $\delta_B$  are undergoing mutual chemical exchange. In the EXSY spectrum we see a set of cross-peaks which are consistent with the reaction scheme of Figure 8. see text for further discussion.

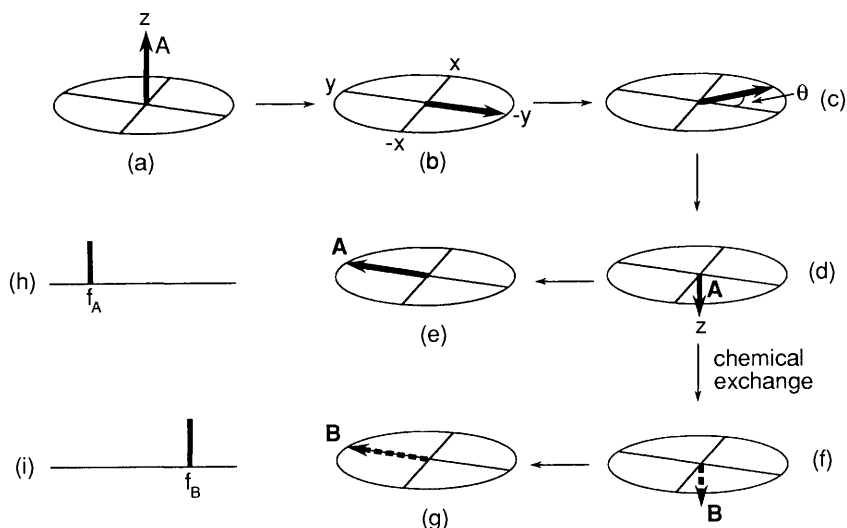


**Figure 10** Vector precession diagrams illustrating the effect of the EXCSY pulse sequence, Figure 9 (a). The experiment starts with magnetization of spin A, indicated as a bold arrow, aligned along the z axis, (a). A  $90^\circ$  pulse rotates the magnetization vector onto the  $-y$  axis, (b) and the vector then precesses in the  $xy$  plane for a time  $t_1$ . At the end of  $t_1$  the vector makes an angle  $\theta = 2\pi f_A t_1$  with the  $-y$  axis, (c). A second  $90^\circ$  pulse rotates the  $-y$  component of the vector (proportional to  $\cos \theta$ ) onto the  $-z$  axis, (d). During the mixing time,  $\tau_{\text{mix}}$ , the molecule may undergo a conformational change which converts spin A into spin B. During such a change the spin 'takes its magnetization with it', as indicated in (f). The final pulse rotates the vector onto the  $y$  axis, (g), where it is detected and gives rise to a signal at  $f_B$ , (i). If no conformational change takes place during the mixing time the vector retains its identity as A and the final pulse gives rise to a signal that is detected at  $f_A$ , (e) and (h). Most importantly, the size of the signal detected at either  $f_A$  or  $f_B$  is proportional to  $\cos \theta$

(iii) A radio-frequency pulse can be applied to rotate these vectors about the  $x$  axis. The angle through which the vector is rotated is called the flip angle. For example, a pulse with a flip angle of  $90^\circ$  rotates the vector from the  $z$  axis to  $-y$ .

(iv) Once in the  $xy$  plane, each vector precesses around the  $z$  axis at a frequency which depends on its chemical shift.

(v) Only magnetization vectors in the  $xy$  plane give rise to a free induction signal.

Imagine a molecule which has just one kind of proton which is undergoing an interconversion, slow on the NMR timescale, between two conformers A and B. In the conventional spectrum two peaks are observed, one for each of the conformers, at shifts  $f_A$  and  $f_B$ . Figure 10 shows the action of the pulse sequence of Figure 9 (a) using vector diagrams and for simplicity only the vector from conformer A is considered. The initial  $90^\circ$  pulse rotates the magnetization vector about the  $x$  axis moving it from  $z$  to  $-y$ , (a) and (b). During  $t_1$  the vector

precesses in the  $xy$  plane so that after  $t_1$  the vector makes an angle of  $2\pi f_A t_1$  with the  $-y$  axis, Figure 10 (c) The second  $90^\circ$  pulse is applied and causes a further rotation about the  $x$  axis This pulse will have no effect on the  $x$  component of the magnetization vector, as this is aligned along the axis about which the pulse acts In contrast, the component along the  $-y$  axis is rotated to the  $-z$  axis If the original vector is of length  $M$ , then the component which is rotated to the  $-z$  axis is of size  $M \cos(2\pi f_A t_1)$ , Figure 10 (d) The component left along the  $x$  axis is of no further interest in the current experiment and its effect can be ignored for the moment

The next event in the pulse sequence is the mixing time,  $\tau_{\text{mix}}$  This time is made long enough so that there is a significant chance of the molecule undergoing a conformational change from A to B Suppose that the molecule under consideration in the previous section does indeed undergo such a change, then the magnetization vector aligned along the  $-z$  axis of size  $M \cos(2\pi f_A t_1)$  remains unaltered by the chemical process, but it is now associated with a spin on a molecule of type B, Figure 10 (f)

The final pulse of the sequence rotates this magnetization from the  $-z$  axis to the  $y$  axis, Figure 10 (e) and (g) The free induction decays from the precessing magnetizations are observed and after Fourier transformation give rise to spectra (h) and (i) For the magnetization which has been transferred from being on molecule A to molecule B during the mixing time the spectrum will show a peak at  $f_B$ , (i), whereas the magnetization which remains on molecule A gives a peak at  $f_A$ , (h) Note, however, that the magnetization that gives rise to both of these signals precessed at  $f_A$  during  $t_1$  The final result of this analysis is to predict the appearance of a cross-peak at  $F_1 = f_A$ ,  $F_2 = f_B$ , and a diagonal peak at  $F_1 = f_A$ ,  $F_2 = f_A$  The cross-peak arises from magnetization that was transferred by chemical exchange during the mixing time, and the diagonal-peak from magnetization that was not transferred

It is appropriate at this point to look in more detail at how the evolution during  $t_1$  effects the signal observed during  $t_2$  From the above analysis it was seen that the  $y$  magnetization present after the last pulse has a size proportional to  $\cos(2\pi f_A t_1)$  in other words the *size* of the signal observed during  $t_2$  depends on the evolution during  $t_1$  For the first increment of  $t_1$  ( $t_1 = 0$ ), the signal will be a maximum, the second increment will have size proportional to  $\cos(2\pi f_A \Delta_1)$ , the third proportional to  $\cos(2\pi f_A 2\Delta_1)$ , the fourth to  $\cos(2\pi f_A 3\Delta_1)$  and so on This modulation of the *amplitude* of the observed signal by the  $t_1$  evolution is illustrated in Figure 11 In the Figure the first column shows a series of free inductions decays that would be recorded for increasing values of  $t_1$  and the second column shows the Fourier transforms of these signals The spectra in this second column clearly show how the amplitude of the line in the spectrum varies with  $t_1$

The final step in constructing the two-dimensional spectrum is to Fourier transform the data along the  $t_1$  dimension This process is also illustrated in Figure 11 Each of the spectra shown in the second column are represented as a series of data points, where each point corresponds to a different  $F_2$  frequency



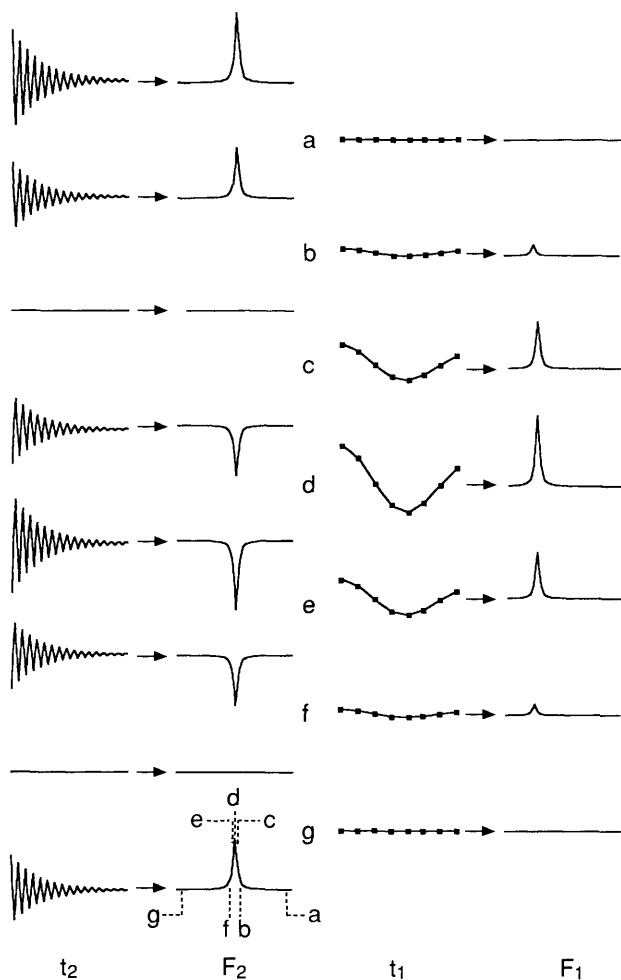


**Figure 11** Illustration of how the modulation of a free induction decay by evolution during  $t_1$  gives rise to a peak in the two-dimensional spectrum. In the left-most column is shown a series of free induction decays that would be recorded for successive values of  $t_1$ ;  $t_1$  increases down the page. Note how the amplitude of these free induction decays varies with  $t_1$ , something that becomes even plainer when the time domain signals are Fourier transformed, as shown in the second column. In practice, each of these  $F_2$  spectra in column two consist of a series of data points. The data point at the same frequency in each of these spectra is extracted and assembled into an interferogram, in which the horizontal axis is the time  $t_1$ . Several such interferograms, labelled a to g, are shown in the third column. Note that as there were eight  $F_2$  spectra in column two corresponding to different  $t_1$  values there are eight points in each interferogram. The  $F_2$  frequencies at which the interferograms are taken are indicated on the lower spectrum of the second column. Finally, a second Fourier transformation of these interferograms gives a series of  $F_1$  spectra shown in the right hand column. Note that in this column  $F_2$  increases down the page, whereas in the first column  $t_1$  increase down the page. The final result is a two-dimensional spectrum containing a single peak

The data point corresponding to a particular  $F_2$  frequency is selected from the spectra for  $t_1 = 0$ ,  $t_1 = \Delta_1$ ,  $t_1 = 2\Delta_1$  and so on for all the  $t_1$  values. Such a process results in a function, called an *interferogram*, which has  $t_1$  as the running variable. Several interferograms, labelled a–g, computed for different  $F_2$  frequencies are shown in the third column of Figure 11. The particular  $F_2$  frequency that each interferogram corresponds to is indicated in the bottom spectrum of the second column. The amplitude of the signal in each interferogram is different, but in this case the modulation frequency is the same. The final stage in the processing is to Fourier transform these interferograms to give the series of spectra which are shown in the right most column of Figure 11. These spectra have  $F_1$  running horizontally and  $F_2$  running down the page. The modulation of the time domain signal has been transformed into a single two-dimensional peak. Note that the peak appears on several traces corresponding to different  $F_2$  frequencies because of the width of the line in  $F_2$ .

In summary, cross-peaks in an EXCSY spectrum arise by magnetization, which has been labelled with evolution at one frequency, being transferred during the mixing time to another spin where it is observed at a different frequency. The information about the frequencies with which the magnetization has evolved during  $t_1$  is encoded into the amplitude of the signals that are observed during  $t_2$ . This encoding is unravelled into a two-dimensional spectrum by double Fourier transformation. All other two-dimensional experiments share this method of modulating the observed signals by the evolution during  $t_1$ .

## 5 NOESY Spectra

This experiment utilizes the same pulse sequence as the EXCSY technique and is essentially based on the same idea. The only difference is that the phenomenon responsible for transfer of  $z$  magnetization between spins during the mixing time is that of *cross relaxation* rather than chemical exchange.<sup>17</sup> Cross relaxation is a special type of interaction that occurs between two spins that share a through space dipole–dipole coupling. It is the phenomenon responsible for the nuclear Overhauser effect (NOE).<sup>12,18,19</sup>

A NOESY spectrum has cross-peaks which show which spins are undergoing mutual cross relaxation and are therefore close in space to one another. Such information is clearly very useful in establishing the three-dimensional shapes of molecules. For technical reasons small and medium sized molecules do not yield good quality NOESY spectra. However, large molecules, such as proteins and DNA fragments, give excellent NOESY spectra which are very widely used in studying the structures of such molecules.<sup>20</sup>

<sup>17</sup> S. Macura and R. R. Ernst, *Mol. Phys.*, 1980, **41**, 95.

<sup>18</sup> J. H. Noggle and R. E. Schirmer, 'The Nuclear Overhauser Effect', Academic Press, 1971.

<sup>19</sup> D. Neuhaus and M. P. Williamson, 'The Nuclear Overhauser Effect in Structural and Conformational Studies', VCH, 1989.

<sup>20</sup> K. Wüthrich, 'NMR of Proteins and Nucleic Acids', Wiley, 1986.

## 6 COSY Spectra

The pulse sequence for recording COSY spectra, such as those already discussed, is shown in Figure 12. It is a particularly simple sequence consisting of just two pulses, but despite this it is not possible to make an adequate description of how cross-peaks arise in a COSY spectrum without recourse to some quantum mechanical calculations. The results of such a calculation will be presented here; a detailed description can be found in several other places.<sup>5,6,8,9,16,21</sup>

A partial explanation of how a COSY spectrum arises can be made using the vector picture introduced in the previous section. For simplicity consider a system of two coupled spins, A and X, and concentrate on the A multiplet which consists of two lines at frequencies  $f_A \pm \frac{1}{2}J_{AX}$ . These two lines can be represented as two vectors and after the first  $90^\circ$  pulse they are both aligned along the  $-y$  axis, Figure 12 (a). The two vectors precess at different frequencies so that at the end of the time  $t_1$  they make angles  $2\pi(f_A + \frac{1}{2}J_{AX})t_1$  and  $2\pi(f_A - \frac{1}{2}J_{AX})t_1$  with the  $-y$  axis, Figure 12 (b). Normally the  $x$  and  $y$  components of these two vectors would be considered, but the quantum mechanical calculations indicate that a different decomposition is appropriate. The vectors are decomposed into four components which have the following arrangements: (1) both vectors aligned along the  $-y$  axis, (2) both vectors aligned along the  $x$  axis, (3) one vector aligned along  $y$  and one along  $-y$ , (4) one vector aligned along  $x$  and one along  $-x$ . The reason for this choice should become clearer as the explanation proceeds. The components numbered (1) and (2) are called *in-phase* magnetization along  $y$  and  $x$  respectively; components (3) and (4) are called *anti-phase* magnetization along  $y$  and  $x$  respectively. This decomposition is indicated in Figure 12 (c).

As with the EXCSY sequence, the size of these different components depends on the angles through which the two vectors have precessed and hence on the frequencies of the two lines. A full quantum mechanical calculation reveals that the second  $90^\circ$  pulse has a different effect on each of the four components. In-phase magnetization along  $x$  is unaffected and evolves during  $t_2$  as a signal giving rise to the A spin doublet. In-phase magnetization along  $y$  is rotated to the  $z$  axis and is therefore no longer observable. Anti-phase magnetization along  $x$  is transferred into a special state called *multiple quantum coherence* which is not observable. Finally, and most importantly, anti-phase magnetization along  $y$  which started out on the A spin is transferred into anti-phase magnetization associated with the X spin. During  $t_2$  this gives a signal which results in an X spin doublet in the spectrum. The fate of the various components are shown in Figure 12 (d).

This last process, known as *coherence transfer*, is responsible for generation of cross-peaks in the COSY spectrum. As its name implies, coherence transfer results in magnetization on the A spin being transferred to the X spin. As in the case of EXCSY, the size of the signal transferred from A to X depends on the evolution

<sup>21</sup> O. W. Sørensen, G. W. Eich, M. H. Levitt, G. Bodenhausen, and R. R. Ernst, *Prog. NMR Spectrosc.*, 1983, 16, 163.

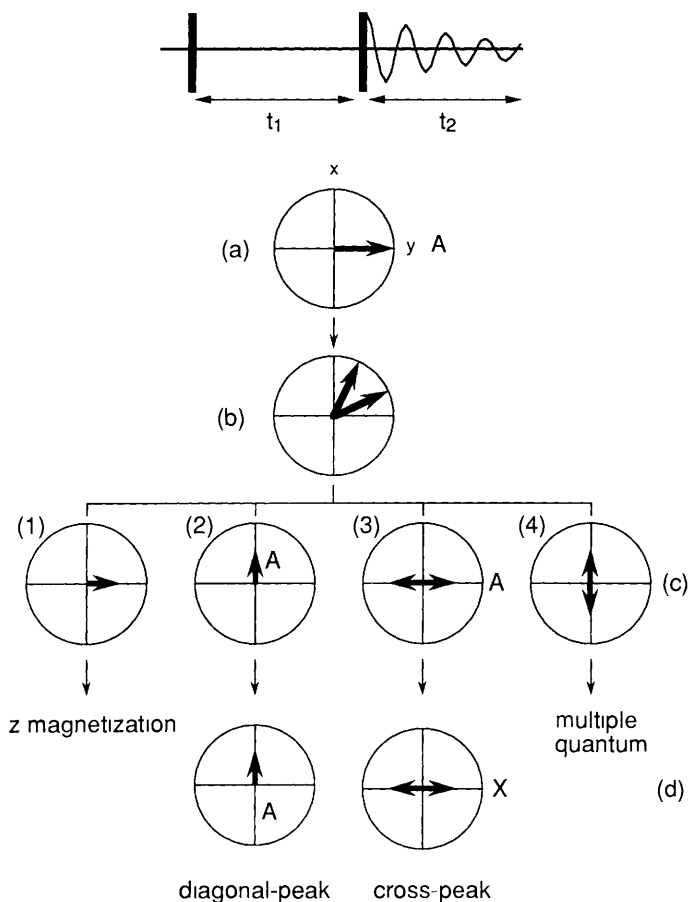


**Figure 12** At the top is shown the pulse sequence used to record two-dimensional COSY spectra and below are vector precession diagrams indicating how the experiment proceeds. The  $A$  spin doublet of an  $AX$  spin system is considered. After the first  $90^\circ$  pulse the two vectors corresponding to the two lines of the doublet are both aligned along the  $-y$  axis (a). After time  $t_1$  they have precessed at different speeds and hence are separated in the  $xy$  plane (b). A full quantum mechanical calculation reveals that the two vectors should be resolved into four components as indicated in (c). Components (1) and (2) have both vectors aligned along the  $-y$  and  $x$  axes respectively and are called in-phase states. Component (3) has the two vectors aligned with one along  $+y$  and one along  $-y$  and likewise (4) has them aligned along  $+x$  and  $-x$ . These are called anti-phase states. The effect of the last pulse can only be deduced from a full quantum mechanical calculation. This shows that component (1) is turned to the  $z$  axis and component (4) becomes multiple quantum coherence both of which are unobservable. Component (2) is unaffected by the pulse and remains associated with the  $A$  spin giving rise to a diagonal-peak multiplet. Component (3) undergoes coherence transfer to the coupled spin  $X$  and gives rise to a cross-peak multiplet in the COSY spectrum.

during  $t_1$  and it is in this way that the observed signal is modulated by the evolution during  $t_1$ .

The details of this calculation reveal some further features of the COSY spectrum which have not been discussed so far. The diagonal peaks result from magnetization that was in-phase just before the last pulse, and remains in-phase after it. This results in all four components in the diagonal peak having the same sign. In contrast, the cross-peaks arise from the transfer of anti-phase magnetization from one spin to another and this results in the cross-peak multiplet having two positive and two negative components arranged on the diagonals of the square. The spectra presented in this review have all been processed and plotted in the *absolute value or magnitude* mode in which the modulus of the (complex) spectral data is displayed.<sup>16</sup> Although this masks the different signs of individual peaks in the spectrum it turns out for a variety of technical reasons to be a convenient way of plotting spectra. Recent developments have now made it more common to process and plot spectra in such a way that this sign information is not lost. Further discussion of this important point is beyond the scope of this review, but is described in detail in reference 22.

## 7 Heteronuclear Correlation Spectra

So far all the experiments described have involved only the proton spectrum, however, it is equally possible to devise two-dimensional experiments which involve other nuclei, for example carbon-13. In this section one such experiment, usually known as 'shift correlation' will be described.<sup>23,24</sup> This experiment gives rise to a spectrum in which the  $F_1$  coordinate of a cross-peak is the proton chemical shift and the  $F_2$  coordinate is the carbon-13 chemical shift. Using such a spectrum the proton assignment of (1) can be used to assign all the carbon-13 resonances.

As with COSY spectra, the method of finding which carbon-13 atoms are joined to which protons is to devise an experiment in which there is coherence transfer from protons to carbon-13. Figure 13 (a) shows one possible pulse sequence that could be used to achieve this. This sequence is just the direct analogue of the COSY experiment, modified so that the pulses affect both the carbon-13 and proton spectra. The reason for needing separate pulses for each type of nucleus is that their resonance frequencies are so widely separated that a single pulse cannot affect both types of nucleus. With virtually all NMR spectrometers it is only possible to record signals from one type of nucleus at a time and it is most usual in these shift correlation experiments to record the signals from carbon-13. Since the aim is to present a spectrum in which the  $F_1$  coordinates of the cross-peaks are proton shifts, the first pulse is applied only to protons. Hence, only proton magnetization evolves during  $t_1$ .

The one-bond carbon-13 proton coupling is typically in the range 120 to 200 Hz and is much larger than any of the long-range couplings between the two nuclei. This fact can be used to make a modification of the pulse sequence of

<sup>22</sup> J. Keeler and D. Neuhaus, *J. Magn. Reson.*, 1985, **63**, 454.

<sup>23</sup> G. A. Morris and R. Freeman, *J. Chem. Soc., Chem. Commun.*, 1978, 684.

<sup>24</sup> A. A. Maudsley, A. Kumar, and R. R. Ernst, *J. Magn. Reson.*, 1977, **28**, 463.

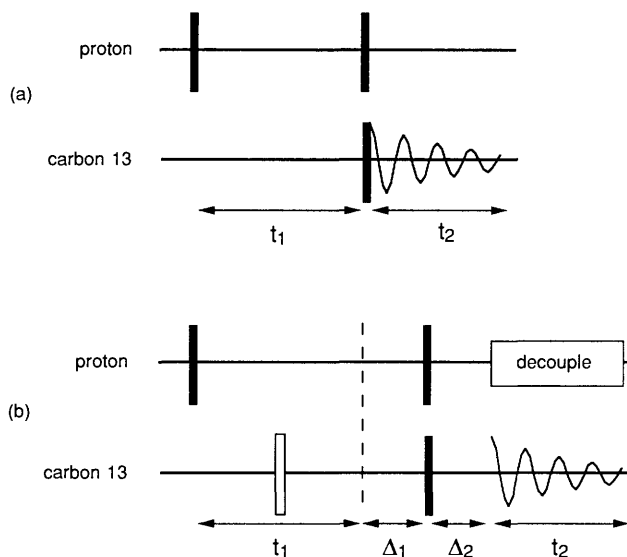


**Figure 13** (a) Shows a simple pulse sequence for recording two-dimensional shift correlation spectra in which the cross-peaks indicate the presence of a coupling between a proton and a carbon-13. The sequence is very similar to that for COSY except that only the carbon-13 signal is observed. This sequence can be modified so that splittings in both  $F_2$  and  $F_1$  due to carbon-13 proton couplings are removed from the spectrum. This is achieved in the  $F_2$  dimension by using broadband proton decoupling during data acquisition and in  $F_1$  by inserting a proton  $180^\circ$  pulse midway in  $t_1$ ; in the figure the  $180^\circ$  pulse is represented by an open box. For reasons described in the text two delays  $\Delta_1$  and  $\Delta_2$  also have to be included in the sequence. (b) These delays should be set to approximately  $1/(2J_{CH})$  where  $J_{CH}$  is a typical value of the carbon-13 proton coupling through which correlations are desired. By setting these delays for a coupling of around 130 Hz only cross-peaks between directly bonded carbon-13 proton pairs will be seen in the spectrum. Such a one-to-one map of directly bound proton vs. carbon-13 shifts is very useful in assignment.

Figure 13 (a) which results in a spectrum which shows only correlations between directly bonded carbon-13 proton pairs. In addition the resulting spectrum is simpler in appearance and has higher sensitivity.

There are two modifications made to the pulse sequence. The first is to add broadband decoupling of the protons during the acquisition time,  $t_2$ . Such decoupling is the normal practice for recording one-dimensional carbon-13 spectra for the reason that it collapses the often complex carbon-13 multiplet to a single sharp line, thereby greatly increasing both sensitivity and resolution. However, in analogy with COSY spectra, the magnetization that has been transferred from protons to carbon-13 by the last two pulses in the sequence is in anti-phase. Applying broadband decoupling to such a state causes the coupling to collapse to zero and thus the two anti-phase lines will cancel one another and no signal will be observed. This problem is circumvented by leaving a suitable delay,  $\Delta_2$ , prior to switching on the decoupler. The simple vector picture can be used to predict the correct value of this delay: the two vectors which represent the lines of

the doublet start out aligned along the  $y$  and  $-y$  axes respectively, and during the delay they evolve through angles  $2\pi(\delta_C + \frac{1}{2}J_{CH})\Delta_2$  and  $2\pi(\delta_C - \frac{1}{2}J_{CH})\Delta_2$  respectively. Thus the angle between the vectors increases by  $2\pi J_{CH}\Delta_2$  during the delay, and it is clear that if  $\Delta_2$  is set to  $1/(2J_{CH})$  this angle will be  $\pi$  at the end of the delay. Thus, after such a delay the vectors have evolved from being in anti-phase ( $180^\circ$  apart) to being in-phase. The decoupler may now be switched on safely.

The second modification is to place a carbon-13  $180^\circ$  pulse in the middle of the  $t_1$  period. It can be shown that such a pulse has the effect of preventing any of the carbon-13 proton couplings causing splittings in the  $F_1$  dimension of the spectrum. However, in order to have any coherence transfer from protons to carbon-13 it is necessary that an anti-phase state is created, and this is achieved by adding a further delay,  $\Delta_1$ , of  $1/(2J_{CH})$  just prior to the last two pulses. The final pulse sequence is shown in Figure 13 (b).

Figure 14 shows the carbon-13 proton shift correlation spectrum of (1) recorded using the pulse sequence of Figure 13 (b). Although the experiment is based on the same ideas as COSY, that of coherence transfer, it looks very different indeed to a COSY spectrum. There are two reasons for this difference: first, the carbon-13 proton couplings have been removed from each dimension so that each cross-peak is a single peak; secondly, the spectrum consists entirely of cross-peaks, the diagonal-peaks have not been recorded because only the carbon-13 signal was observed. In principle, proton-proton couplings are still present in the  $F_1$  dimension, but the resolution is often not adequate to reveal them.

The shift-correlation spectrum of (1) enables the proton assignment previously determined to be used to assign the carbon-13 spectrum, since each cross-peak indicates a directly bonded carbon-13 proton pair. In more complex cases where the proton assignment is only partially known, the correlation spectrum can be used along with the COSY to aid in the assignment of both the carbon-13 and proton spectra. It is also possible to devise modified carbon-13 proton shift correlation spectra that show cross-peaks between long-range coupled pairs of nuclei; such spectra are of great utility in assigning the quaternary carbons in a molecule.

Recently, it has been shown that there are considerable advantages in recording these carbon-13 proton shift correlation spectra with observation of the *proton* signal rather than the carbon-13.<sup>25-27</sup> Such experiments are generally known as *inverse experiments* as they are recorded in the opposite way from what was the normal practice. These inverse experiments benefit from the fact that, due to the higher resonance frequency of protons than carbon-13, a given number of protons give rise to a much larger signal than the same number of carbon-13 atoms. Thus the sensitivity of the inverse experiment is much higher, an advantage which enables such experiments to be carried out successfully on larger molecules than was previously possible.

<sup>25</sup> L. Müller, *J. Am. Chem. Soc.*, 1979, **101**, 4481.

<sup>26</sup> A. Bax, R. H. Griffey, and B. L. Hawkins, *J. Magn. Reson.*, 1983, **55**, 301.

<sup>27</sup> J. Cavanagh, C. A. Hunter, D. N. M. Jones, J. Keeler, and J. K. M. Sanders, *Magn. Reson. Chem.*, 1988, **26**, 867.

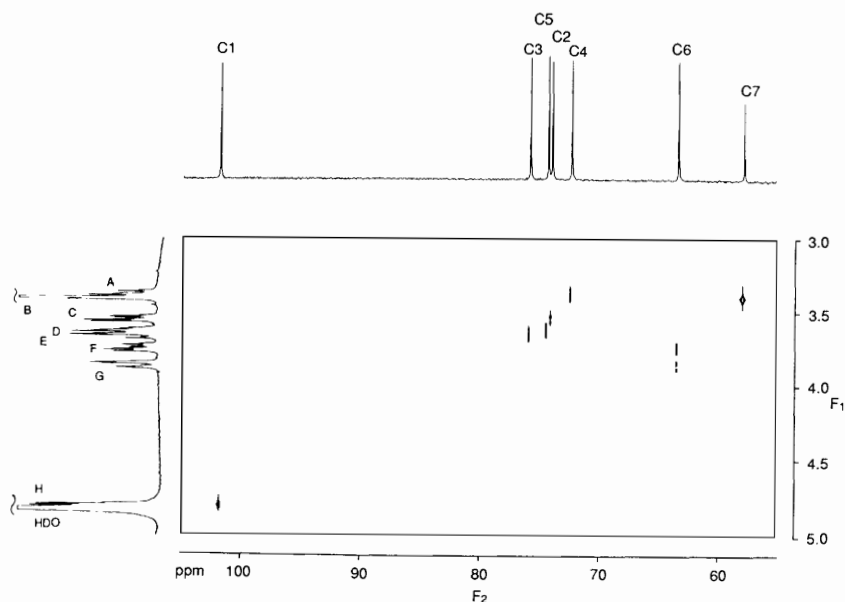


**Figure 14** Carbon-13 proton shift correlation spectrum of (1) obtained using the pulse sequence of Figure 13(b). The delays  $\Delta_1$  and  $\Delta_2$  have been set so that only correlations through one-bond carbon-proton couplings are seen. The conventional carbon-13 and proton spectra are plotted along the  $F_2$  and  $F_1$  axes respectively. Using the assignment of the proton spectrum found from the COSY spectrum, a complete assignment of the protonated carbons is a trivial task from this spectrum

## 8 General Features of Two-Dimensional Spectroscopy

It was noted in the introduction that a very large number of two-dimensional NMR experiments have been devised, but it turns out that in day-to-day use the COSY, EXCSY (NOESY) and shift correlation experiments account for well over two-thirds of all spectra recorded. The other experiments are generally somewhat more complex and have been devised to solve particular complex problems of assignment.

It is often supposed that two-dimensional spectroscopy is a fundamentally insensitive technique. This erroneous point of view arises from the observation that recording a two-dimensional experiment involves recording a one-dimensional spectrum for each value of  $t_1$ . Inspection of Figure 11 reveals why this point of view is incorrect. After the first Fourier transformation with respect to  $t_2$  the modulated signal appears in each spectrum which was recorded for each  $t_1$  value. However, after the second Fourier transformation with respect to  $t_1$  this signal is concentrated into one peak in the two-dimensional spectrum, rather than being spread out as it was before transformation. This concentration of the signal achieved by the double Fourier transformation shows that the signal-to-noise ratio in the two-dimensional spectrum is much better than the signal-to-



noise ratio achieved for a spectrum recorded at a particular  $t_1$  value. In fact, the final signal-to-noise ratio of the two-dimensional spectrum is closely related to the signal-to-noise ratio that would be achieved in an equivalent one-dimensional experiment which lasted for the same total duration as the whole two-dimensional experiment.<sup>28,29</sup>

Many two-dimensional experiments are recorded using pulse sequences that contain several radio-frequency pulses. As described in the previous sections, such pulses are used to achieve coherence transfer or to rotate magnetization between the  $z$  axis and the  $xy$  plane. It turns out that radio-frequency pulses tend to be rather indiscriminate in the way they affect the spins, and in addition to achieving the desired transformation they may also move magnetization to unwanted places or generate unwanted multiple quantum coherences. These processes can give rise to peaks in the two-dimensional spectrum that may cause confusion or may obscure other wanted peaks. In addition, imperfections in the spectrometer can also give rise to further peaks. Often, it is possible to select just the desired processes, and hence the desired peaks in the spectrum, by a technique known as *phase cycling*.<sup>30,31</sup> This involves repeating the pulse sequence (for a fixed value of  $t_1$ ) with a systematic variation of the phases of the pulses in the sequence. The way in which phase cycles are devised is beyond the scope of this review, but suffice it to say that such cycles are essential for many two-dimensional experiments.

The techniques described in this work have been illustrated by reference to proton and carbon-13 spectra but the experiments are equally applicable to other nuclei such as nitrogen-15, boron-11, phosphorus-31, and fluorine-19. Two-dimensional NMR has been widely used to study the structures of molecules containing these less common nuclei. It has not been possible in this review to discuss two very important applications of two-dimensional spectroscopy. The first has been the study of multiple quantum spectra.<sup>32</sup> These spectra arise from transitions which are not allowed by the normal selection rules for NMR, but as has been alluded to above it is possible to generate multiple quantum coherence with a suitable pulse sequence. Such multiple quantum coherences cannot be observed directly but their evolution can be followed using two-dimensional spectroscopy. A large number of applications have been found for multiple quantum spectra, ranging from spectral simplification and editing to relaxation studies. The second area that has not been mentioned is the application of two-dimensional NMR to the study of solid materials; such materials have radically different spectra to those encountered in liquid samples but despite this two-dimensional spectroscopy is used in a similar way to aid in assignment and interpretation.<sup>33</sup>

<sup>28</sup> W. P. Aue, P. Bachmann, A. Wokaun, and R. R. Ernst, *J. Magn. Reson.*, 1978, **29**, 523.

<sup>29</sup> M. H. Levitt, G. Bodenhausen, and R. R. Ernst, *J. Magn. Reson.*, 1984, **58**, 462.

<sup>30</sup> G. Bodenhausen, H. Kogler, and R. R. Ernst, *J. Magn. Reson.*, 1984, **58**, 370.

<sup>31</sup> J. Keeler in 'Multinuclear Magnetic Resonance in Liquids and Solids—Chemical Applications', ed. P. Granger and R. K. Harris, NATO ASI Series C: Vol. 322, Kluwer (Dordrecht), 1990.

<sup>32</sup> G. Bodenhausen, *Prog. NMR Spectrosc.*, 1981, **14**, 137.

<sup>33</sup> B. Blümich and H. W. Spiess, *Angew. Chem., Int. Ed. Engl.*, 1988, **27**, 1655.

*Acknowledgements.* I am grateful to Adrian Davis and Julia Richardson for carefully reading the manuscript and making numerous suggestions for improvements, and to Dr. Jeremy Sanders for encouragement and invaluable advice on the selection of example compounds.